Observations of a Quantum Symmetry Restriction in the Rovibrationally Inelastic Scattering of Glyoxal†

Samuel M. Clegg‡ and Charles S. Parmenter*

Department of Chemistry, Indiana University, Bloomington, Indiana 47405

Received: March 13, 2000; In Final Form: June 9, 2000

Rovibrationally inelastic scattering of S_1 *trans*-glyoxal (CHOCHO, 12 modes) by H_2, D_2, and He is explored experimentally. Explicit attention is given to a state-to-state inelastic channel that is predicted to be forbidden on account of quantum symmetry restrictions in the symmetric top approximation for glyoxal ($\kappa = -0.99$). This channel is 0^0, $K' = 0 \rightarrow 7^1$, $K' = 0$, where 0^0 is the S_1 zero-point level, 7^1 is the CHO−CHO torsional fundamental, and K' is the quantum number for angular momentum about the top axis. After $S_1 \leftarrow S_0$ pumping of the initial state, inelastic scattering to the set of final states 7^1, $K' = n$ that includes the $\Delta K' = 0$ channel is monitored by dispersed fluorescence. Relative cross sections for the rovibrational transitions are obtained for inelastic scattering by H_2 ($E_{c.m.} = 650$ and 1170 cm^{-1}), D_2 (750 cm^{-1}), and He (750 and 1220 cm^{-1}) to final states with K' ranging from 0 to 15. The predicted prohibition of the $\Delta K' = 0$ channel does not occur, but that channel is present with its scattering cross section reduced to only about half of the value expected if no symmetry effects were present. The partial relaxation of the quantum symmetry prohibition may plausibly be attributed to the small asymmetric top character of this near symmetric top molecule.

1. Introduction

One of the prominent distinctions between the treatments of intramolecular versus intermolecular vibrational energy flow in polyatomic molecules concerns the role of quantum state symmetry. Molecular symmetry restrictions are central to the anharmonic vibrational interactions that underlie the collision-free flow of vibrational energy in polyatomic molecules. Accordingly, discussions of state symmetries inevitably accompany theoretical treatments of this intramolecular vibrational redistribution, IVR.[1−5] In contrast, intermolecular vibrational energy flow, or collisional vibrational energy transfer (VET), has historically been modeled without reference to restrictions arising from issues of state symmetry. The extent to which treatments such as the SSH-T theory[6−8] or the related Tang−Parmenter rules[9,10] have had semiquantitative success emphasizes the fact that state-to-state VET propensities largely escape molecular symmetry constraints, and consequently, symmetry is not a common part of VET discussions.

When the VET experiment moves from vibrational to rovibrational state resolution, symmetry considerations come to the fore, but even then, only occasionally. The few VET studies that comment on state symmetries all involve state-to-state transitions between rovibronic states, whether actually resolved in the observations or implicitly invoked in the discussion. Many concern rovibrational energy transfer between perturbed states high in the vibrational manifold of C_2H_2.[11,12] Perhaps most notable are those between states of different spin symmetry for which the transitions appear to break the g/u symmetry prohibition.[13,14] Another example involves rovibrational transitions in CO_2 where the accompanying ΔJ rotational changes display propensities for preserving overall rovibrational symmetry.[15]

The present paper concerns an energy transfer symmetry restriction occurring in a larger molecule, glyoxal, CHOCHO, with 12 modes, for which many competing rovibrational channels can be resolved in crossed beam inelastic scattering experiments. The scattering has also been explored with fully quantal three-dimensional scattering calculations[16−19] that generally have good fidelity with the experimental results.[20−27] The calculations predict that a strong state symmetry prohibition occurs for one of the channels.[17,18] This effect did not appear, however, in the scattering data of H_2[20,21,23]or He,[22,23] and on this issue the experiments and theory are in disagreement. We now present new inelastic scattering data obtained with experimental improvements that allow a better view of the channel that is involved in the predicted symmetry effect.

The glyoxal inelastic scattering channels are seen with help from Figure 1 that shows some of the rovibrational energy levels in the $S_1(^1A_u)$ state. Laser S_1-S_0 pumping is used to prepare the 0^0 level with $K' = 0$ in the symmetric top approximation (with $\kappa = -0.99$, glyoxal is almost a prolate top). The quantum number K is related to the angular momentum about the top axis (Figure 1). Overall rotation associated with J is not resolved in these experiments. Rotationally inelastic scattering occurs to K' states within the zero-point level and rovibrationally inelastic scattering reaches K' states within the fundamental $\nu'_7 = 233$ cm^{-1}. The rotational structure of dispersed S_1-S_0 fluorescence is used to detect these single-collision destination states with K-state resolution. Relative cross sections for the competition among inelastic scattering channels are extracted by computer simulation of the fluorescence spectrum produced by those molecules that have undergone inelastic scattering.[23,27]

The rovibrational channel of specific interest is that with $\Delta K' = 0$, namely the 0^0, $K' = 0 \rightarrow 7^1$, $K' = 0$ scattering event. With the symmetric top approximation for glyoxal, the azimuthal and vibrationally close-coupled, infinite-order sudden scattering approach (AVCC-IOS) predicts that this transition is symmetry forbidden.[17,18] The prohibition originates in the close-coupled

† Part of the special issue "C. Bradley Moore Festschrift".

‡ Present address: Department of Geophysical Sciences, The University of Chicago, 5734 S. Ellis Ave., Chicago, IL 60637.

10.1021/jp000948f CCC: $19.00 © 2000 American Chemical Society
Published on Web 07/28/2000

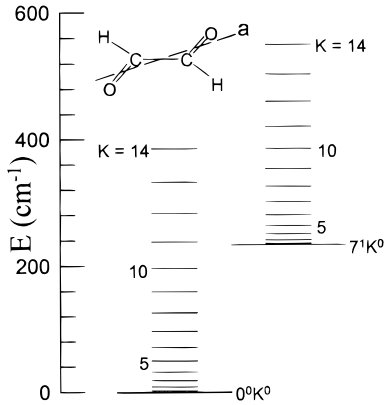

Figure 1. $K = J$ rotational energy levels within the 0^0 and 7^1 vibrational levels that can be observed in the inelastic scattering from the 0^0, $K' = 0$ (or 0^0K^0) level of glyoxal with a display of the principal top "*a*" axis of planar glyoxal in the symmetric top approximation.

matrix element that involves integration over the products of the initial and final vibrational states, the symmetry-adapted *K*-state eigenfunctions and the interaction potential for a collision of a symmetric top with an atom. For the $\Delta K' = 0$ transition, the matrix element contains the product of an even and an odd function, the integral of which is zero. For those rovibrational transitions with $\Delta K' > 0$, at least some components of the matrix element are nonzero and symmetry influences are predicted to disappear. Thus, the main symmetry prohibition is predicted to occur for the single rovibrational channel $\Delta K = 0$.

With the exception of the $\Delta K' = 0$ rovibronic scattering, the scattering calculations calculations[16−19] for state-resolved rotational and rovibrational inelastic scattering are in semiquantitative agreement with the data.[20−27] The match of the predictions with the data holds broadly, encompassing experiments with several scattering gases and with scattering from four different initial S_1 rovibrational states of glyoxal. Thus, the AVCC-IOS and the symmetric top approximations for S_1 glyoxal appear generally valid. Given these predictive successes, the experimental finding that $\Delta K' = 0$ is the most probable rovibrational channel[23] rather than a forbidden channel becomes even more intriguing.

A possible contributor to the mismatch between the data and calculations concerns the symmetric top approximation for glyoxal in the calculations. Asymmetric top characteristics in near-symmetric top molecules are expressed most prominently for low *K*-states[28] so that while the symmetric top approximation may work satisfactorily for most inelastic scattering channels, problems may arise for the low ΔK channels, with the $\Delta K = 0$ channel being an extreme example. On the other hand, the data for low ΔK rovibrational channels may also have spectroscopic liabilities, and their assay is difficult. The spectroscopic signature of the 0^0, $K' = 0 \rightarrow 7'$, $K' = 0$ channel lies in a region of the fluorescence spectrum that is congested relative to those for the higher $\Delta K'$ rovibronic channels. Additionally, the spectral simulation used previously to extract the relative scattering cross sections from that fluorescence region was made with a symmetric top program.[23]

Subsequent developments in both the experimental apparatus and the data analysis now set the stage for further experimental exploration of the rovibrational scattering channels involved in the predicted symmetry restrictions. The fluorescence resolution has been improved nearly 3-fold with concomitant improvement of the signal-to-noise so that better definition of the $\Delta K' = 0$ rovibrational channel is obtained. The crossed beam apparatus has been fitted with a new nozzle mount which allows one to change the angle between the sample and target molecular beams from 55° to 180°. This angle control allows one to tune the relative velocity of the molecular beams and to select desired kinematics while preserving the molecular beam expansion characteristics. Improvements in the data analysis have also been made, of which perhaps the most important is a switch to an asymmetric top spectral simulation program. The changes give improved simulation accuracy, especially for emission from states with low K' values. With these advances, we have obtained new data to characterize the rovibrational scattering in the set of channels 0^0, $K' = 0 \rightarrow 7^1$, $K' = n$, where *n* ranges from 0 to as high as 15. The new data encompass scattering of H_2 and of He at each of two center-of-mass collision energies, $E_{c.m.,}$ plus scattering of D_2 at one $E_{c.m.}$ value.

TABLE 1: Glyoxal 0^0K^0 + M Kinematic Conditions

target gas	scattering angle (deg)	v_{rel} (m/s)	$E_{c.m.}$ (cm^{-1})	$p_{c.m.}$ ($\times 10^{-24}$ kg/s)
H_2	90	2810	640	9.08
H_2	180	3790	1170	12.3
He	90	2190	750	13.6
He	130	2790	1220	17.3
D_2	90	2190	750	13.6

2. Experimental Procedures

Inelastic scattering is observed in the intersection of pulsed supersonic beams. The sample beam is a seeded He beam carrying seven mole percent glyoxal. The target beam is obtained from the expansion of pure H_2, He, or D_2. Glyoxal is pumped to its 0^0, $K' = 0$ level with J' in the range of 0−10 by a laser tuned to the 0 S_1-S_0 $K' = 0 \leftarrow K'' = 1$ subbandhead. The confluence of the 0.3 cm^{-1} laser bandwidth with overlapping rotational structure in the subbands results in an S_1 rotational population of at least 85% $K' = 0$ while the remaining pumped molecules are in as many as four neighboring K' levels. The rovibronic structure of S_1 fluorescence in the region of the S_1-S_0 7^1_1 band is observed by imaging the fluorescence from a 1.7 m monochromator equipped with Princeton Instruments intensified charge-coupled device (ICCD) detection.

Details of the beam conditions, laser pumping, and fluorescence collection have been described elsewhere.[29,23] Two modifications of the earlier procedure require comment. The first is incorporation of adjustable beam intersection angles as opposed to the fixed 90° intersection of previous reports. In addition to observations of scattering by H_2, D_2, and He at 90° intersection, here we include data for scattering of H_2 and He at an intersection angle of 180° and 130°, respectively. The collision kinematics for all five scattering experiments are summarized in Table 1.

The second modification has been a switch from photomultiplier (PMT) detection of the dispersed fluorescence signal to detection by an ICCD. The change to ICCD detection allows us to improve the fluorescence resolution to 0.75 cm^{-1} from the 2.0 cm^{-1} resolution obtained with the PMT while simultaneously improving the signal-to-noise.

3. Results

The 0^0, $K' = 0 \rightarrow 7^1$, $K' = n$ rovibrationally inelastic scattering channels are observed by the rotational structure in the 7^1_1 fluorescence band. As described in earlier reports, the H_2/D_2/He beam is kept off on alternate laser pulses so that interleaved spectra with and without scattering are acquired. The difference of these spectra is fluorescence from only those

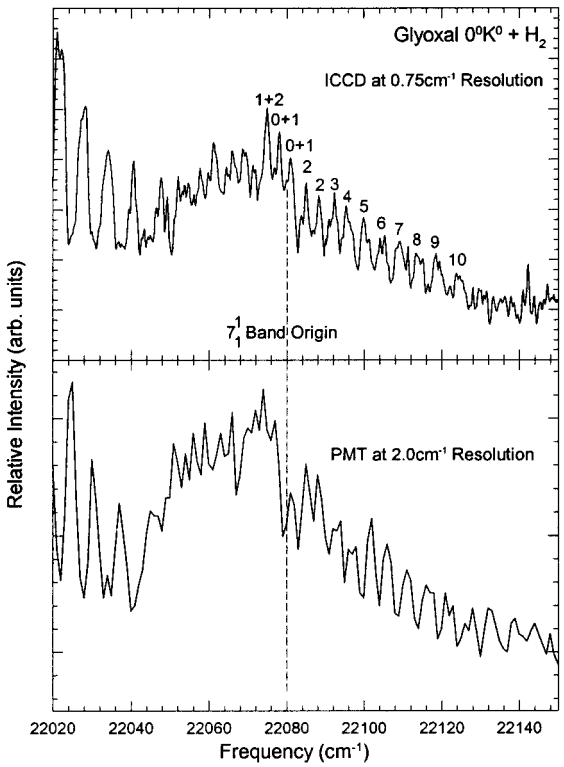

Figure 2. A comparison of glyoxal (0^0, $K' = 0$) + H_2 fluorescence rovibrational scattering spectra in the 7_1^1 band region at the 0.75 cm^{-1} resolution achieved with ICCD detection and at 2.0 cm^{-1} resolution from PMT detection. The 0.75 cm^{-1} spectrum is annotated with the principal K' level or levels that contribute to the subband maxima. The prominent maxima below 22040 cm^{-1} are from high K' levels in the 0 band that are populated by rotationally inelastic scattering. For these experiments, $E_{c.m.} = 650$ cm^{-1}.

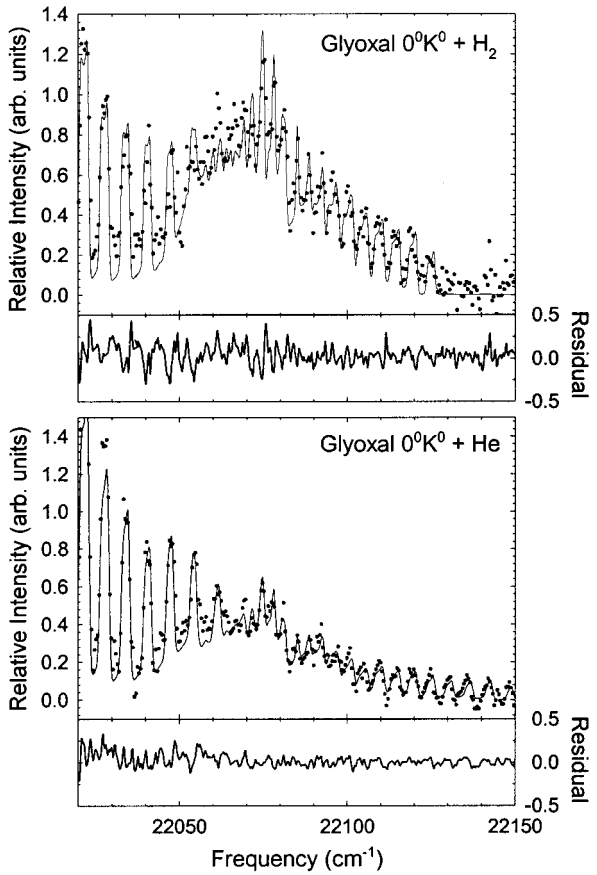

Figure 3. Rovibrational scattering spectra (dots) in the 7_1^1 band region for glyoxal (0^0, $K' = 0$) scattering of H_2 ($E_{c.m.} = 650$ cm^{-1}) or He ($E_{c.m.} = 750$ cm^{-1}) with fits by simulation (lines). The two spectra use different arbitrary units.

molecules that have undergone inelastic scattering. We term the result a "scattering" spectrum.

A typical scattering spectrum is shown in Figure 2. The symmetric top $\Delta K = \pm 1$, $\Delta J = 0,\pm 1$ selection rules cast emission from a given K' level into six subbands. The ^{P}P, ^{P}Q, and ^{P}R subbands occur as congested emission to the red of the 7_1^1 band origin. The ^{r}P, ^{r}Q, and ^{r}R lines occur to the blue of the 7_1^1 origin. For $K' \geq 3$, this blue structure appears with prominent ^{r}R subband heads identified in Figure 2 with the K' identity of the emitting levels. Emission from $K' = 0$, 1, or 2 occurs near the 7_1^1 band origin, and in this region, lines from different K' levels contribute substantially to a single subband maximum. The K' identities of the dominant contributors for the various maxima are noted in the figure.

Figure 2 additionally shows a comparison of spectra obtained with PMT and ICCD detection. The improvement in detail from the 0.75 cm^{-1} ICCD resolution vs the 2.0 cm^{-1} PMT resolution is readily apparent. The spectral region carrying information about emission from the 7^1, $K' = 0$ states of special interest for this study benefits particularly from the improved resolution.

The relative cross sections for rovibrationally inelastic scattering to the states 7^1, $K' = n$ are obtained from simulation of the scattering spectrum. As described elsewhere,[23,27] enough is known about glyoxal spectroscopy and photophysics so that the simulation can be made with only two adjustable parameters. One accommodates the profile of the rotational subbands. It plays a secondary role in the cross section determinations, and its nature is described elsewhere.[23,27] The other is the set of relative K' populations of the scattered molecules. Populations are adjusted for the best spectral replication. Since the scattering is primarily that of single collision events, the set of relative populations that emerges from the simulation is also the set of relative scattering cross sections.

The quality of the simulations is representative of the examples shown in Figure 3. The simulation procedure using the symmetric top approximation is described in detail elsewhere.[23,27] Two improvements have been used in the simulations for the present work. While the symmetric top approximation with inclusion of centrifugal stretching provides an excellent replication for most states reached in the scattering, the approximation is potentially troublesome for emission from $K' = 0$, 1, or 2. The problems were moot for the earlier experiments with 2.0 cm^{-1} PMT resolution where structure from those states is poorly resolved (see Figure 2). To accommodate the improved resolution and our particular interest in low K' populations for the present study, we have switched to an asymmetric rotor simulation program. The functionality of the simulation program is the same as described previously[23,27] except the intensities are calculated as a function of the more accurate asymmetric frequencies rather than at the symmetric top frequencies. The best fit simulation is determined to be the one with the smallest sum of the square of the residuals.

The sets of relative rovibrationally inelastic scattering cross sections for the five experiments involving the H_2, D_2, and He are reported in Table 2 and plotted in Figure 4. The error bars associated with the cross sections in Figure 4 reflect *only* the uncertainty in the best fit spectrum. The uncertainties are calculated with a nonlinear least-squares routine provided by incorporating STARPAC (the Standard Time Series and Regression Package) into the simulation program.[30] More realistic

TABLE 2: Relative Cross Sections for the Rovibrationally Inelastic Scattering of Glyoxal (0^0, $K' = 0$) → (7^1, $K' = n$) by H_2, D_2, or He at Specified $E_{c.m.}$[a]

	$\sigma(H_2)$		σ(He)		$\sigma(D_2)$
n	$E_{c.m.} = 650\ cm^{-1}$	$E_{c.m.} = 1170\ cm^{-1}$	$E_{c.m.} = 750\ cm^{-1}$	$E_{c.m.} = 1220\ cm^{-1}$	$E_{c.m.} = 750\ cm^{-1}$
0	1.2	1.1	1.6	1.4	1.4
1	2.9	2.9	2.8	2.9	3.3
2	2.1	2.1	1.7	1.8	1.6
3	1.6	1.9	2.2	2.0	1.5
4	1.6	1.6	1.7	1.8	1.8
5	1.8	1.5	1.6	1.5	1.8
6	1.3	1.1	0.9	1.3	1.1
7	1.2	1.2	1.1	1.4	1.0
8	0.9	0.7	0.9	0.8	0.7
9	1.0	0.9	0.9	0.6	1.3
10	0.7	0.4	0.6	0.8	0.6
11		0.6	0.5	0.2	0.2
12		0.3	0.4	0.6	0.4
13		0.4	0.5		0.3
14		0.2			
15		0.2			

[a] The final K' state is specified as n. The cross section sets are normalized by setting the sum of channels with $n = 1-5$ to a common value.

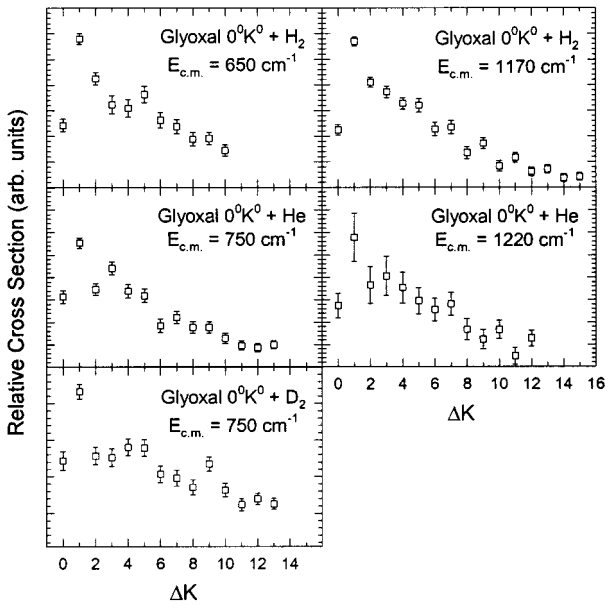

Figure 4. Relative cross sections for rovibrationally inelastic scattering from 0^0, $K' = 0$ glyoxal plotted against ΔK (which is $K' = n$ of Table 2).

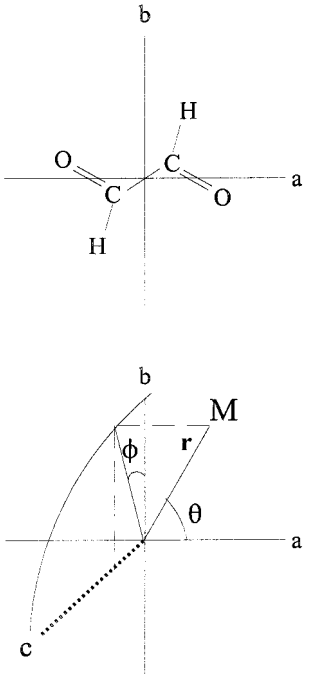

Figure 5. (top) Principal inertial axes of glyoxal. The molecule lies in the *a*,*b* plane. The *a* axis is the top or unique axis. (bottom) The coordinate system for the scattering formulation where **r** is the vector from the glyoxal center of mass to the approaching particle M with the polar angle θ defined from the top axis of glyoxal and the azimuthal angle ϕ defined from the molecular plane.

uncertainties are in the range of 20−30%. This range is observed in the reproducibility of cross sections occurring in various pairs of independent experiments.

4. Discussion

The prediction that the 0^0, $K' = 0 \rightarrow 7^1$, $K' = 0$ rovibrationally inelastic scattering channel is symmetry forbidden is a consequence of the rotational and vibrational wave functions employed in the AVCC-IOS calculations.[17−19] While in this paper we focus our experimental efforts on a quantum symmetry effect in scattering from the initial level 0^0, $K' = 0$, quantum symmetry effects have been predicted for several other initial levels. Since these effects do not depend on details of the intermolecular potential surface, the theoretical predictions apply in principle to all target gases. The predictions concerned specifically the scattering of glyoxal from H_2, He, and Ar.[17−19] A brief recapitulation of the theory responsible for the quantum symmetry effect is discussed in the first part of this section. Additional insights into the AVCC-IOS calculations may be found in the original papers.[16−19,31−34]

The quantum symmetry argument can be summarized with the help of Figure 5 that displays the principal axes of glyoxal and the coordinate system for the interacting pair glyoxal + M.[17] The approach of the collision partners is defined by the center of mass separation vector **r** with a polar angle θ with respect to the top axis of glyoxal (the *a* axis) and an azimuthal angle ϕ with respect to the molecular plane (the *a*−*b* plane).

The rovibrationally inelastic scattering cross sections for v'', $K'' \rightarrow v'$, K' channels are contained in the AVCC-IOS S-matrix elements whose development involves coupled-channel matrix elements of the form

$$V^{v''K''t''}_{v'K't'}(r,\theta) = \int\int_0^{2\pi} g_{v'}(q)\, h^{t'}_{k'}(\phi) V_I(r,q,\theta,\phi) g_{v''}(q) h^{t''}_{k''}(\phi)\, d\phi\, dq \quad (1)$$

The integral is over the initial and final molecular states and the interaction potential $V_I(r,q,\theta,\phi)$ where $g_v(q)$ is the vibrational wave function in harmonic normal coordinates q and h (ϕ) is the molecular rotational wave function. With the sudden approximation for the slow rotation, the symmetric top wave function becomes that for the fast rotation only. It is composed of basis functions that are symmetry adapted to the molecular plane with the form

$$h_k^1 = \cos k\phi/\sqrt{\pi(1+\delta_{0k})} \tag{2a}$$

$$h_k^2 = \sin k\phi/\sqrt{\pi} \tag{2b}$$

where k is the projection of j on the top axis.[18,19]

The forbiddance of the 0^0, $K' = 0 \rightarrow 7^1$, $K' = 0$ channel derives from the integration over ϕ that requires each element in the integrand to have definite symmetry with respect to the plane of the molecule.[17−19] The potential V_I is necessarily totally symmetric. The vibration υ_7 is an out-of-plane mode so that the vibrational wave function $g_v(q)$ is symmetric or antisymmetric with respect to the molecular plane for even or odd valves of the vibrational quantum number, respectively. With $K' = 0$ in both the initial and final scattering states, the symmetry-adapted rotational wave function reduces to a constant. Accordingly, the initial state molecular wave function with $\upsilon_7' = 0$ is symmetric with respect to the molecular plane, whereas the final state wave function with $\upsilon_7' = 1$ is antisymmetric. Integration over ϕ sets up an even−odd integral that vanishes, and thus the 0^0, $K' = 0 \rightarrow 7^1$, $K' = 0$ scattering channel is symmetry forbidden.

When the initial rotational state is $K' = 0$, the $\Delta K' = 0$ channel would be symmetry forbidden for any even−odd combination of υ_7 states. More generally, the $\Delta K' = 0$ channel is forbidden for an odd change from $K' = 0$ in any out-of-plane vibration. The corresponding channel would be allowed for even−even or odd−odd transitions in these modes. On the other hand, all in-plane vibrations are necessarily symmetric with respect to the molecular plane so that the symmetry restriction would not pertain to scattering transitions in these modes. For example, consider the in-plane modes υ_5 and υ_{12}. In these cases, rather than being forbidden, the $\Delta K' = 0$ channel is actually the most probable in the predicted $0^0 \rightarrow 5^1$ and $0^0 \rightarrow 12^1$ rovibrational scattering from the initial state $K' = 0$. Unfortunately, the only observed vibrationally inelastic channels are those with $\Delta\upsilon_7 = \pm 1$ so that other experimental tests for these predictions are out of reach.

The rotational wave function for the final states with $K' > 0$ contain basis functions from both eqs 2a and 2b and consequently have symmetric as well as antisymmetric components. Scattering from 0^0, $K' = 0$ to any state 7^1, $K' > 0$ is thus allowed without symmetry restrictions.

On account of the small asymmetric top character of glyoxal, one might expect the inelastic scattering cross sections for $\Delta K' = 0$ channels of the rovibrational scattering discussed above to be markedly smaller than those for $\Delta K' > 0$ transitions but not zero. The asymmetric top character of glyoxal may be expected to relax prohibitions as extreme as a $\Delta K' = 0$ "selection rule" even though the symmetric top approximation remains valid for many other aspects of the inelastic scattering. The actual "$K' = 0$" asymmetric top wave function is approximated by inclusion of symmetric top components with $K' \neq 0$. These components will preclude the integral from vanishing. The selection rule for $\Delta K' = 0$ inelastic scattering is thus modified to a propensity rule.

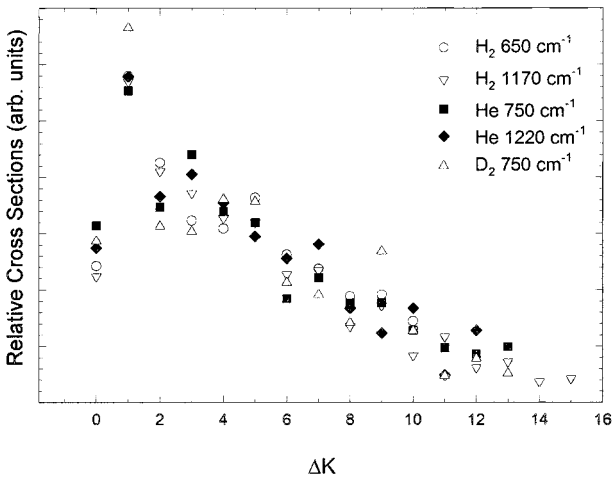

Figure 6. Relative cross sections for the rovibrationally inelastic glyoxal scattering 0^0, $K' = 0 \rightarrow 7^1$, $K' = n$ by H_2 ($E_{c.m.} = 650$ and 1170 cm^{-1}), by He ($E_{c.m.} = 750$ and 1220 cm^{-1}) and by D_2 ($E_{c.m.} = 750$ cm^{-1}) plotted against the change $\Delta K'$ in angular momentum quantum number for the top axis. The plots use the normalized arbitrary units of Table 2 that allow facile comparison of the inelastic scattering experiments.

A classical analogy exists for the $\Delta K' = 0$ rovibrational restriction. As noted in discussions accompanying the early glyoxal experiments [20,21] and the theory,[17−19] excitations of rotation about the top axis and of the υ_7 CHO−CHO torsion are closely connected. The torsion and rotation are out-of-plane and in-plane versions of the same motion so that classical trajectories that excite one will also be most effective in exciting the other. Thus, the symmetric top $\Delta K = 0$ quantum symmetry restriction also occurs classically in the form of a low probability for a vibrational transition without rotational excitation.

The predicted $\Delta K' = 0$ restriction in the 0^0, $K' = 0 \rightarrow 7^1$, $K' = n$ rovibronic scattering channels has been explored in the present work with five distinct experiments. They involve inelastic scattering of 0^0, $K' = 0$ glyoxal by H_2, D_2, and He at the kinematic conditions listed in Table 1. The outcome of the inelastic scattering is given by the relative cross sections for scattering into the set of channels involving the final states 7^1, $K' = n$ as plotted in Figure 4 and listed in Table 2.

In Figure 4, the data are plotted separately against $\Delta K'$ for each experiment. The $\Delta K' = 0$ channel is always measurable, but it occurs with a cross section reduced by about a factor of 2 from the value of the $\Delta K' = 1$ channel. By this means, the display shows that the $\Delta K' = 0$ selection rule has, in effect, become a propensity rule for reduced inelastic scattering probability.

An alternative plot of the five sets of cross sections is given in Figure 6 where a common normalization has been used for facile comparisons of the rovibrationally inelastic scattering characteristics. The display shows that the competition among inelastic scattering channels is similar for all five scattering experiments. The diminished $\Delta K' = 0$ cross section is a consistent part of this correspondence. All the data are consistent with a quantum restriction for the $\Delta K' = 0$ channel.

The close correspondence of the five scattering experiments suggests that the rovibrational channel *competition* is relatively insensitive to variations in the interaction potential energy surface (PES) or the kinematic factors provided by the different scattering gases and differing kinematic values. This insensitivity is similar to that occurring in pure rotationally inelastic scattering where the cross section distributions for scattering from 0^0, $K' = 0$ glyoxal by H_2 and those by the full rare gas series are all

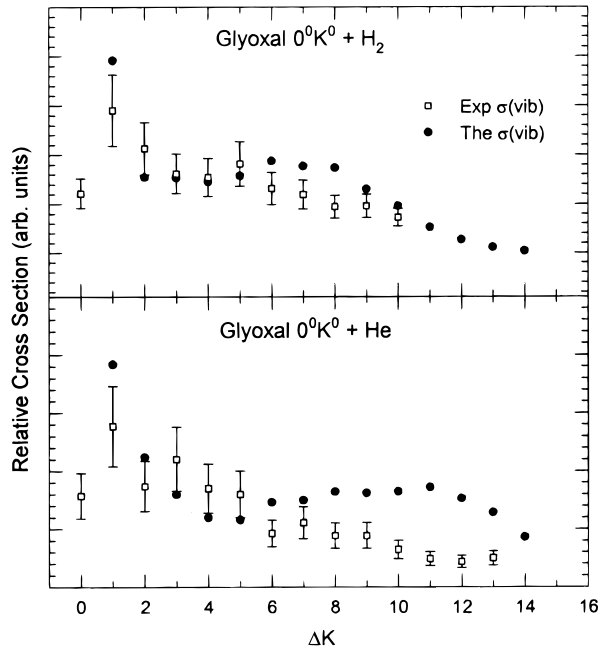

Figure 7. A comparison of the calculated[17−19] vs experimental relative rovibrationally inelastic cross sections for the scattering of H_2 ($E_{c.m.}$ = 650 cm^{-1}) and He ($E_{c.m.}$ = 750 cm^{-1}) from glyoxal 0^0, $K' = 0 \rightarrow 7^1$, $K' = n$. The calculated and experimental cross sections have been normalized to each other with different normalizations for H_2 and He. In this display, as distinct from Figure 4, the experimental cross sections carry 25% error bars to reflect more realistically the uncertainties experienced with repetition of specific scattering experiments.

nearly coincident.[27] Despite the more extreme range of PES and kinematic characteristics found in the rotational experiments, the rotational channel competition is always the same except for a few channels with the light gases where H_2 and He run out of the angular momentum needed for the higher $\Delta K'$ transitions. Discussion of the phenomenon accompanies those data.[27]

Figure 7 contains a comparison of our new H_2 and He rovibrational cross sections ($E_{c.m.}$ = 650 cm^{-1} for H_2; 750 cm^{-1} for He) with the AVCC-IOS predictions. Other than the predicted symmetry restriction on the $\Delta K' = 0$ channel, the most notable distinction between theory and experiment is the appearance of a predicted secondary maximum in the distribution. The experimental cross section plots in Figure 4 containing the error bars established by the spectral simulation statistics might suggest that secondary maxima occur also in the experimental distributions. In Figure 7, these cross sections are plotted with the more realistic 25% error bars that are indicated by the reproducibility of separate experiments. In this representation, it is seen that the data are not sufficiently refined to establish the presence of secondary maxima.

The display in Figure 7 is somewhat misleading with respect to the general quality of the theory. A comparison of theoretical and experimental cross section distributions that encompasses *both* rotationally and rovibrationally inelastic scattering with earlier H_2 and He data appears elsewhere.[23−25] The theory reproduces well both the rotational distributions and the overall magnitude of the rovibrational cross sections. The latter is a particularly demanding test of the AVCC-IOS scattering theory. It is clear that use of the symmetric top approximation is appropriate for glyoxal, except of course for the $\Delta K' = 0$ rovibrational symmetry restriction. The problems with the detailed shape of the rovibrational cross section distribution have been noted earlier.[17−19]

Acknowledgment. We are grateful for the financial support of the National Science Foundation. Discussions with Prof. G. J. Kroes, Dr. T. A. Stone, M. Duca, and Dr. M. J. Weida as well as installation of the ICCD detector and input into the simulation program by Dr. Weida have been most helpful.

References and Notes

(1) Nesbitt, D. J.; Field, R. W. *J. Phys. Chem.* **1996**, *100*, 12735−12756.
(2) Quack, M.; Kutzelnigg, W. *Ber. Bunsen-Ges. Phys. Chem.* **1995**, *99*, 231.
(3) Lehmann, K. K.; Scoles, G.; Pate, B. H. *Annu. Rev. Phys. Chem.* **1994**, *45*, 241.
(4) Timbers, P. J.; Parmenter, C. S.; Moss, D. B. *J. Chem. Phys.* **1994.**, *100*, 1028−1034.
(5) Holtzclaw, K. W.; Parmenter, C. S. *J. Chem. Phys.* **1986**, *84*, 1099−1118.
(6) Schawrtz, R. M.; Slawsky, Z. I.; Herzfeld, K. F. *J. Chem. Phys.* **1952**, *20*, 1591.
(7) Schawrtz, R. M.; Herzfeld, K. F. *J. Chem. Phys.* **1954**, *22*, 767−773.
(8) Tanczos, F. I. *J. Chem. Phys.* **1956**, *25*, 439−447.
(9) Parmenter, C. S.; Tang, K. *ACS Symp. Ser.* **1977**, *56*, 175−178.
(10) Tang, K. Y.; Parmenter, C. S. *J. Chem. Phys.* **1983**, *78*, 3922−3934.
(11) Orr, B. J. *Chem. Phys.* **1995**, *190*, 261−278.
(12) Saarinen, M.; Permogorov, D.; Halonen, L. *J. Chem. Phys.* **1999**, *110*, 1424−1428.
(13) Payne, M. A.; Milce, A. P.; Frost, M. J.; Orr, B. J. *Chem. Phys. Lett.* **1997**, *265*, 244−252.
(14) Milce, A. P.; Orr, B. J. *J. Chem. Phys.* **1996**, *104*, 6423−6434.
(15) Flynn, G. W.; Weston, R. E. J. *J. Phys. Chem.* **1993**, *97*, 8116−8127.
(16) Clary, D. C.; Dateo, C. E. *Chem. Phys. Lett.* **1989**, *154*, 62−66.
(17) Kroes, G.-J.; Rettschnick, R. P. H.; Dateo, C. E.; Clary, D. C. *J. Chem. Phys.* **1990**, *91*, 287−311.
(18) Kroes, G.-J.; Rettschnick, R. P. H.; Clary, D. C. *Chem. Phys.* **1990**, *148*, 359−379.
(19) Kroes, G.-J.; Rettschnick, R. P. H. *J. Chem. Phys.* **1991**, *94*, 360−370.
(20) Butz, K. W.; Du, H.; Krajnovich, D. J.; Parmenter, C. S. *J. Chem. Phys.* **1987**, *87*, 3699−3700.
(21) Butz, K. W.; Du, H.; Krajnovich, D. J.; Parmenter, C. S. *J. Chem. Phys.* **1988**, *89*, 4680−4691.
(22) Gilbert, B. D.; Parmenter, C. S.; Krajnovich, D. J. *J. Phys. Chem.* **1994**, *98*, 7116−7122.
(23) Gilbert, B. D.; Parmenter, C. S.; Krajnovich, D. J. *J. Chem. Phys.* **1994**, *101*, 7423−7439.
(24) Gilbert, B. D.; Parmenter, C. S.; Krajnovich, D. J. *J. Chem. Phys.* **1994**, *101*, 7440−7450.
(25) Parmenter, C. S.; Clegg, S. M.; Krajnovich, D. J.; Lu, S.-P. *Proc. Natl. Acad. Sci.* **1997**, *94*, 8387−8392.
(26) Clegg, S. M.; Gilbert, B. D.; Lu, S.-p.; Parmenter, C. S. In *Highly Excited Molecules Relaxation, Reaction, and Structure*, 678th ed.; Mullin, A. S., Schatz, G. C., Eds.; ACS Symposium Series 678; American Chemical Society: Washington, DC, 1997; pp 237−250.
(27) Clegg, S. M.; Burrill, A. B.; Parmenter, C. S. *J. Phys. Chem. A* **1998**, *102*, 8477−8485.
(28) Townes, C. H.; Schawlow, A. L. *Microwave Spectroscopy*; Dover Publications: New York, 1975.
(29) Krajnovich, D. J.; Butz, K. W.; Du, H.; Parmenter, C. S. *J. Chem. Phys.* **1989**, *92*, 7705−7724.
(30) Donaldson, J. R.; Tryon, P. V. The Standards Time Series And Regression Package; National Institute of Standards and Technology: Boulder, CO, 1990.
(31) Clary, D. C. *J. Chem. Phys.* **1984**, *81*, 4466−4473.
(32) Clary, D. C. *J. Chem. Phys* **1986**, *86*, 813−821.
(33) Clary, D. C.; Green, S. *Chem. Phys.* **1987**, *112*, 15−22.
(34) Clary, D. C. *J. Phys. Chem.* **1987**, *91*, 1718−1727.